Acta Crystallographica Section C
Crystal Structure Communications
ISSN 0108-2701

$ZnTe_6O_{13}$, a new $ZnO–TeO_2$ phase

Jalal M. Nawash,[a] Brendan Twamley[b]* and Kelvin G. Lynn[a]

[a]Center for Materials Research, Materials Science Program, Washington State University, Pullman, WA 99164, USA, and [b]University Research Office, University of Idaho, Box 443010, Moscow, ID 83844-3010, USA
Correspondence e-mail: btwamley@uidaho.edu

Received 18 May 2007
Accepted 5 June 2007
Online 14 July 2007

Our investigations into the $ZnO–TeO_2$ system have produced a new phase, zinc(II) hexatellurium(IV) tridecaoxide, $ZnTe_6O_{13}$, with trigonal ($R\bar{3}$) symmetry, synthesized by repeated heating and cooling to a maximum temperature of 1053 K. The asymmetric unit consists of a Zn atom coordinated in a distorted octahedral fashion by two unique tellurium(IV) oxide units that form trigonal–bipyramidal TeO_4 and TeO_{3+1} corner- and edge-shared polyhedra. Except for the Zn and an O atom, which occupy 6*c* positions, all atoms occupy 18*f* general positions.

Comment

The established phase diagram of the $ZnO–TeO_2$ system has three crystalline compositions, *viz*. $ZnTeO_3$ (Hanke, 1967) at low TeO_2 mole percent, $Zn_2Te_3O_8$ (Hanke, 1966) at higher TeO_2 mole percent, and the recently reported Zn_3TeO_6 (Weil, 2006). Glassy compositions are of current electronic and photonic research interest (*e.g.* Nukui, 2001; Bürger *et al.*, 1992; Öveçoğlu *et al.*, 2004). The title compound, (I), was obtained unexpectedly by repeated melting and cooling of the 21:79 mole percent $ZnO–TeO_2$ mixture normally used to produce the mixed-phase TeO_2 and $Zn_2Te_3O_8$. This mole percent is used to achieve the lowest melting mixture at the eutectic point and reduces the evaporation of TeO_2 during the melt. The additional melting cycles (the last at very high temperature), as well as the additional cooling under an O_2 flow, may have contributed to the formation of the new $ZnTe_6O_{13}$ phase.

The space group of (I), according to systematic absences, may be *R*3, $R\bar{3}$, *R*32, *R*3*m* or $R\bar{3}m$; however, subsequent structure and least-squares refinement indicated that the correct space group is $R\bar{3}$. Fig. 1 shows the full coordination environment around each metal center. There are two unique Te^{IV} atoms in the asymmetric unit and the complete coordination environment around each is generated by symmetry [Te1, symmetry code: (i) $-x+\frac{2}{3}, -y+\frac{1}{3}, -z+\frac{1}{3}$, O2; Te2, symmetry code: (ii) $-y+1, x-y+1, z$, O4; see Table 1]. Both are four-coordinate trigonal–bipyramidal (tbp), *i.e.* TeO_4, with a stereochemically active lone pair of electrons, a common motif in tellurate(IV) structures. The environment around Te1

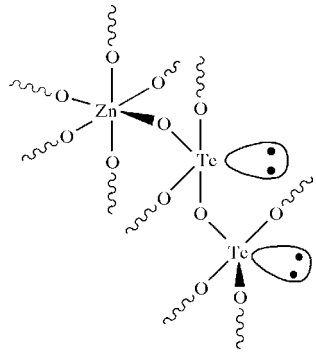

(I)

(see Table 1), although compressed, is similar to that in α-TeO_2 [Te—O = 1.919 and 2.087 Å, and apical O—Te—O = 163.9° (Leciejewicz, 1961); Te—O = 1.903 (20) and 2.082 (23) Å, and apical O—Te—O = 168.5 (13)° (Lindqvist, 1968)]. However, the coordination around Te2 is similar to the TeO_{3+1} coordination found in $ZnTe_3O_8$, $CuTe_2O_5$ (Hanke *et al.*, 1973) and $CuTe_3O_8$ (Feger *et al.*, 1999), with three similar Te—O distances and the fourth significantly longer (see Table 1). In (I), the tbp TeO_4 polyhedra are both corner linked equatorial to apical for both Te1–Te2 and Te2–Te2 polyhedra, and edged shared for Te1–Te1 polyhedra. Corner-sharing TeO_4 polyhedra are seen in α-TeO_2, but both corner- and edged-shared TeO_4 polyhedra are seen in $ZnTeO_3$ and $ZnTe_3O_8$.

The coordination environment around the unique Zn atom after symmetry generation (see Table 1) is a highly distorted octahedron with *trans* O—Zn—O angles of *ca* 163°. Three of the O atoms are corner linked to Te1 polyhedra and the other three are corner linked to Te2 polyhedra, all to equatorial O atoms. Three Te2 units and atom Zn1 form an adamantyl-type substructure. Three Te1 units and atom Zn1 form a 'paddle

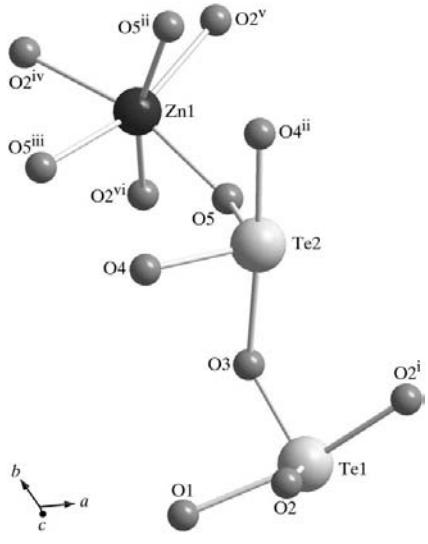

Figure 1
The full coordination environment around each unique metal center in the asymmetric unit of (I). Symmetry codes are as given in Table 1.

  DOI: 10.1107/S0108270107027412

wheel' arrangement with oxygen-bridged O2—Te1—O2 atoms (see Fig. 2). The complete packing superstructure consists of a bilayer of tellurium oxide linked by the Te1—O2 bridging units. These bilayers are connected *via* the Zn atoms.

The bulk material was examined by powder X-ray diffraction. The pattern, shown in Fig. 3, indicates that there is a mixture of phases compared with the calculated pure phase, $ZnTe_6O_{13}$, which is shown as an overlay. A simulated powder pattern using *CrystalDiffract* (Palmer, 2007) shows that the bulk composition consists of 54:46% $ZnTe_6O_{13}/Zn_2Te_3O_8$, with no occurrence of α-TeO_2. The composition of the new phase was also confirmed using a Camebax MBX electron-probe microanalyzer with wavelength dispersive spectroscopy (WDS) on polished sections. Compositional distribution between (I) and $Zn_2Te_3O_8$ is shown in a backscattered electron image in Fig. 4.

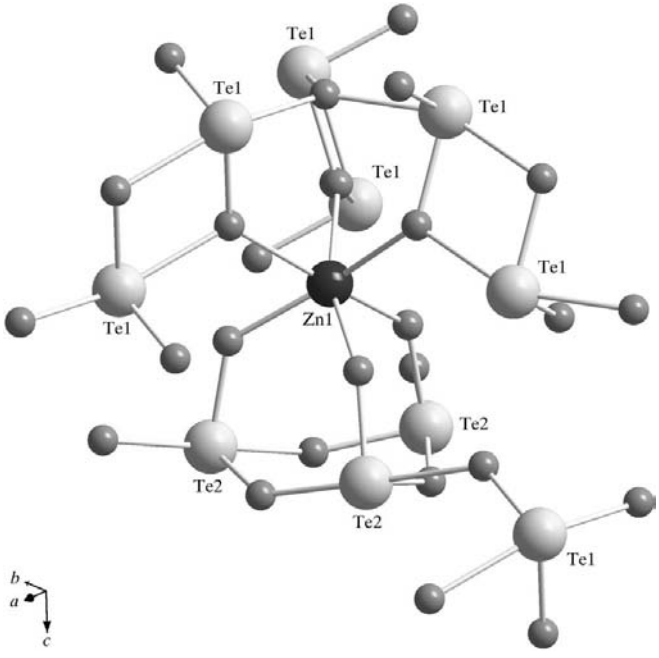

Figure 2
The partial unit cell (coordination completed) drawn parallel to the hexagonal axis [001], showing the arrangement of the tbp TeO_4 units.

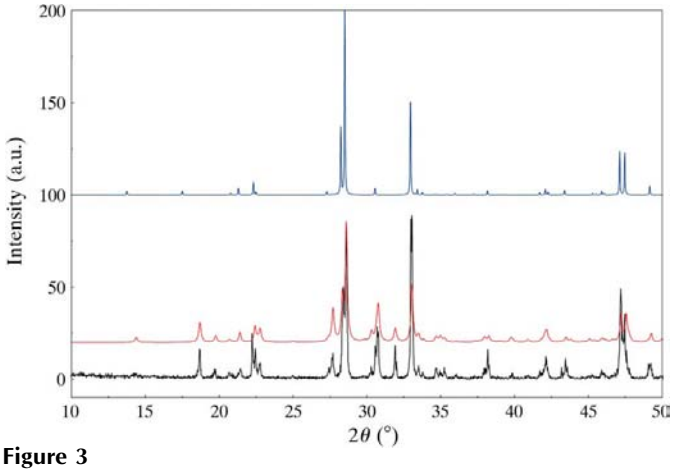

Figure 3
Powder X-ray diffraction overlay pattern for bulk composition (lower scan), calculated mixed composition (middle scan) and calculated pure $ZnTe_6O_{13}$ phase (upper scan) using Cu $K\alpha$ radiation.

Figure 4
A representative backscattered electron image. The black background is the glass substrate. The pale-gray (yellow in the electronic version of the paper) area is $ZnTe_6O_{13}$ and the mid-gray (brown) area is $Zn_2Te_3O_8$ (composition confirmed by WDS).

Experimental

ZnO and TeO_2 powders (Alpha Aesar, 99.999% purity) were mixed in a ZnO:TeO_2 mole percentage of 21:79% using a jar mill with a total average mixing time of 15 h. The mixed powder was placed in a platinum crucible and calcined. The calcined powder was melted and frozen in a radiofrequency furnace several times with (*a*) a maximum temperature of 939 K and a cooling rate of 7 K h^{-1} in air with an O_2 flow, (*b*) a maxmimum temperature of 958 K and a cooling rate of 12 K h^{-1} in air only, (*c*) a maximum temperature of 923 K and a cooling rate of 30 K h^{-1} in air, and (*d*) a maximum temperature of 1053 K and a cooling rate of 48 K h^{-1} in air, and finally cooled at a rate of 2 K h^{-1} with an axial temperature gradient of 60 K cm^{-1} (Bridgman technique: Stockbarger, 1936; King *et al.*, 1996; Rajendran & Mellen, 1987) to room temperature.

Crystal data

$ZnTe_6O_{13}$
M_r = 1038.97
Trigonal, $R\overline{3}$
a = 10.1283 (9) Å
c = 18.948 (3) Å
V = 1683.3 (3) $Å^3$
Z = 6
Mo $K\alpha$ radiation
μ = 17.55 mm^{-1}
T = 86 (2) K
0.13 × 0.06 × 0.02 mm

Data collection

Bruker–Siemens SMART APEX diffractometer
Absorption correction: multi-scan (*SADABS*; Bruker, 2002)
T_{min} = 0.204, T_{max} = 0.705
8273 measured reflections
679 independent reflections
659 reflections with $I > 2\sigma(I)$
R_{int} = 0.033

Refinement

$R[F^2 > 2\sigma(F^2)] = 0.020$	62 parameters
$wR(F^2) = 0.060$	6 restraints
$S = 1.12$	$\Delta\rho_{max} = 0.73$ e Å^{-3}
679 reflections	$\Delta\rho_{min} = -0.69$ e Å^{-3}

Table 1
Selected geometric parameters (Å, °).

O1—Te1	2.1244 (7)	Te2—O4^{ii}	2.026 (4)
O2—Te1	1.936 (4)	O5—Zn1	2.061 (4)
O2—Te1^{i}	2.168 (4)	Zn1—O5^{ii}	2.061 (4)
O3—Te1	1.851 (4)	Zn1—O5^{iii}	2.061 (4)
O3—Te2	2.204 (4)	Zn1—O2^{iv}	2.175 (4)
O4—Te2	1.922 (4)	Zn1—O2^{v}	2.175 (4)
O5—Te2	1.857 (4)	Zn1—O2^{vi}	2.175 (4)
O3—Te1—O2	101.77 (18)	O5^{ii}—Zn1—O2^{iv}	99.42 (17)
O1—Te1—O2^{i}	154.71 (18)	O5^{iii}—Zn1—O2^{iv}	75.45 (17)
O5—Te2—O4^{ii}	94.34 (17)	O5—Zn1—O2^{iv}	162.97 (17)
O4^{ii}—Te2—O3	176.87 (16)	O5^{iii}—Zn1—O2^{v}	162.97 (17)
O5^{ii}—Zn1—O5	96.17 (15)	O5^{ii}—Zn1—O2^{vi}	162.97 (17)
O5^{iii}—Zn1—O5	96.17 (15)		

Symmetry codes: (i) $-x+\frac{2}{3}, -y+\frac{1}{3}, -z+\frac{1}{3}$; (ii) $-y+1, x-y+1, z$; (iii) $-x+y, -x+1, z$; (iv) $-y+\frac{1}{3}, x-y+\frac{2}{3}, z-\frac{1}{3}$; (v) $x+\frac{1}{3}, y+\frac{2}{3}, z-\frac{1}{3}$; (vi) $-x+y+\frac{1}{3}, -x+\frac{2}{3}, z-\frac{1}{3}$.

Data collection: *SMART* (Bruker, 2003); cell refinement: *SAINT-Plus* (Bruker, 2003); data reduction: *SAINT-Plus*; program(s) used to solve structure: *XS* in *SHELXTL* (Bruker, 2003); program(s) used to refine structure: *XL* in *SHELXTL*; molecular graphics: *DIAMOND* (Brandenburg, 1998); software used to prepare material for publication: *publCIF* (Westrip, 2007).

The authors are grateful to Scott B. Cornelius for his assistance in microprobe measurements. The diffraction facility was established at the University of Idaho with the assistance of the NSF–EPSCoR program and the M. J. Murdock Charitable Trust, Vancouver, WA, USA. This research was sponsored by Space Missile and Defense Command (SMDC), contract No. DASG60-02-C-0084.

Supplementary data for this paper are available from the IUCr electronic archives (Reference: IZ3022). Services for accessing these data are described at the back of the journal.

References

Brandenburg, K. (1998). *DIAMOND*. Version 3.0. Crystal Impact GbR, Bonn, Germany.
Bruker (2002). *SADABS*. Version 2.03. Bruker AXS Inc., Madison, Wisconsin, USA.
Bruker (2003). *SMART* (Version 5.630), *SAINT-Plus* (Version 6.45a) and *SHELXTL* (Version 6.14). Bruker AXS Inc., Madison, Wisconsin, USA.
Bürger, H., Kneipp, K., Hobert, H. & Vogel, W. (1992). *J. Non-Cryst. Solids*, **151**, 134–142.
Feger, C. R., Schimek, G. L. & Kolis, J. W. (1999). *J. Solid State Chem.* **143**, 246–253.
Hanke, K. (1966). *Naturwissenschaften*, **53**, 273–273.
Hanke, K. (1967). *Naturwissenschaften*, **54**, 199–199.
Hanke, K., Kupčik, V. & Lindqvist, O. (1973). *Acta Cryst.* B**29**, 963–970.
King, S. E., Dietrich, H. B., Henry, R. L., Katzer, D. S., Moore, W. J., Philips, G. W. & Mania, R. C. (1996). *IEEE Trans. Nucl. Sci.* **43**, 1376–1380.
Leciejewicz, J. (1961). *Z. Kristallogr.* **116**, 345–353.
Lindqvist, O. (1968). *Acta Chem. Scand.* **22**, 977–982.
Nukui, A. (2001). *J. Non-Cryst. Solids*, **255**, 293–295.
Öveçoğlu, M. L., Özalp, M. R., Özen, G., Alten, F. & Kalem, V. (2004). *Key Eng. Mater.* **264–268**, 1891–1894.
Palmer, D. C. (2007). *CrystalDiffract.* Version 1.1.2. Crystalmaker Software Ltd, Oxfordshire, England.
Rajendran, S. & Mellen, R. (1987). *J. Cryst. Growth*, **85**, 130–135.
Stockbarger, D. C. (1936). *Rev. Sci. Instrum.* **7**, 133–136.
Weil, M. (2006). *Acta Cryst.* E**62**, i246–i247.
Westrip, S. P. (2007). *publCIF*. In preparation.